

PRELIMINARY STUDY OF INJECTION TRANSIENTS IN THE TPS STORAGE RING

C. H. Chen[†], Y. C. Liu, J. Y. Chen, M. S. Chiu, F. H. Tseng, S. Fann, C. C. Liang, C. S. Huang, T. Y. Lee, B. Y. Chen, H. J. Tsai, G. H. Luo and C. C. Kuo
 National Synchrotron Radiation Research Center, Hsinchu, 30076, Taiwan

Abstract

An optimized injection efficiency is related to a perfect match between the pulsed magnetic fields in the storage ring and transfer line extraction in the TPS. However, misalignment errors, hardware output errors and leakage fields are unavoidable. We study the influence of injection transients on the stored TPS beam and discuss solutions to compensate these. Related simulations and measurements will be presented.

INTRODUCTION

The Taiwan Photon source (TPS) is one of the most advanced synchrotron light source around the world and has operated since completion of the phase-I commissioning with insertion devices, superconducting cavities and a beam current up to 400 mA [1]. The TPS is a 3 GeV synchrotron facility with design parameters compiled in Table 1. Its booster (BR) and storage rings (SR) share the same tunnel. The septum magnets in the transfer line between the BR and SR have to deflect the beam by about 120 mrad within very limited space. The septa parameters are listed in Table 2. The pulsed magnetic fields from two septum magnets create significant leakage fields and eddy currents which can influence the stored beam during beam injection. The basic requirements of a top-up injection are perfect injection efficiency to reduce the excess radiation and suppress orbit fluctuation during injection. In order to reach these two requirements as much as possible, we will present the efforts in reduction stray fields from the septa and minimization the perturbation of stored beam by optimizing the operation condition of injection kicker.

Synchrotron light sources utilizing pulsed magnets in their injection schemes face beam perturbations during injection. At the NewSUBARU, they found eddy currents in injection beam pipes, in support arms and circulating beam duct. Y. Shoji et al. [2] broke the current loops to reduce these stray currents, which are interfering with the horizontal deflection of the injection beam. P. Lebasque et al. [3] applied a full-sine shape current pulse to simultaneously compensate the delayed eddy currents at SOLEIL in addition to shielding screens on the stored beam path to reduce magnetic stray fields. They further installed mu-metal foils surrounding the stored beam chamber and ground connected it with braided copper conductors in order to eliminate induction currents from septum magnets [4].

Table 1: Design Parameters of TPS Storage Ring

energy	3 GeV
circumference	518.4 m
RF frequency	499.655 MHz
natural emittance	1.6 nm-rad
beam current	500 mA
lifetime time	> 10 hours
tune ν_x/ν_y	26.16/14.24

Table 2: Operational Parameters of SR Septum Magnets

	septum 1 (upstream)	septum 2 (downstream)
septum length (m)	1	
pulse duration (μ sec)	370	
pulse shape	half-sine	
peak voltage (V)	397	392
peak current (A)	8733	8706
peak operation field (T)	0.7274	0.6243
peak design field (T)	0.6283	0.5550
septum thickness (mm)	3	
inner chamber size (mm^2)	20×13	
chamber thickness (mm)	0.4	

SEPTUM MAGNET AND EDDY CURRENT

The septum magnets of the TPS are excited by a half-sine pulse to deflect the electron beam into the storage ring. There is an up- and down-stream septum magnet in the transfer line bending the beam by 3.6° and 3.18° , respectively. The operational septum field is larger than the design value due to the stray field counteracting the main field by inducing eddy currents in the septum chamber. The specifications and performance of the storage ring injection (SRI) septa are listed in Table 2.

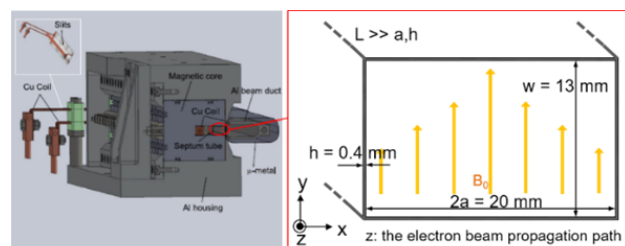


Figure 1: Schematic view of the septum magnet in the transfer line of the TPS [5], the septum vacuum chamber is shown enlarged on the right-hand side.

[†] chen.chiahsiang@nsrc.org.tw

The septum field follows a half-sine wave and the magnetic field B_y is a function of time expressed by Eq. (1)

$$B_y(t) = B_0 \sin\left(\frac{\pi t}{T}\right), \quad 0 < x < 2a, 0 < t < T, \quad (1)$$

where B_0 is the peak magnetic field in the septum, T is the width of the half-sine, $2a$ is the long side dimension of the vacuum chamber, w is the height of the vacuum chamber and h is the thickness of the vacuum chamber walls.

The eddy current is induced by the pulsed septum field forming a loop in the vacuum chamber top or bottom wall and is from Faraday's law of electromagnetic induction Eq.(2)-(7) [6] given by

$$\oint \vec{E} \cdot d\vec{l} = -\frac{\partial}{\partial t} \int \vec{B} \cdot d\vec{A} \quad (2)$$

$$\begin{aligned} \oint \vec{E} \cdot d\vec{l} &= 2 \int_0^{L_B} \vec{E} \cdot d\vec{l} + 2 \int_{-a}^a \vec{E} \cdot d\vec{l} \\ &= 2EL_B + 4Ea \approx 2EL_B \quad (L.H.S.) \end{aligned} \quad (3)$$

$$-\frac{\partial}{\partial t} \int \vec{B}_y(t) \cdot d\vec{A} = 2\dot{B}_y aL \quad (R.H.S.), \quad (4)$$

where L_B is the vacuum chamber length, L is the septum magnet length, and $L \gg a, w, h$ is the vacuum chamber length. Because of the similarity between Eq. (3) and (4), the induction electric field and the current can be expressed by Eq. (5) and (6), respectively. Opposite eddy currents, induced both on top and bottom, are counteracted symmetrically. The total current is equal to the product of the field with the conductivity and chamber wall cross section.

$$E = \dot{B}a \frac{L}{L_B}, \quad (5)$$

$$\begin{aligned} I(t) &= \sigma \dot{B}_y a (2wh + 4h^2) \frac{L}{L_B} \\ &= \sigma a (2wh + 4h^2) B_0 \frac{\pi}{T} \frac{L}{L_B} \cos\left(\frac{\pi t}{T}\right) \end{aligned} \quad (6)$$

The septum vacuum chamber is made of stainless steel type 304, with an electric resistivity of $7.2 \times 10^{-7} \Omega \cdot m$ and a conductivity σ of $1.39 \times 10^6 A/V \cdot m$. The current loop is simplified as a loop in the upstream septum magnet in Fig. 2(b), where L_B is about 1 m and the peak to peak eddy current can be calculated by Eq. (7).

$$\begin{aligned} I_p &= \sigma a (2wh + 4h^2) B_0 \frac{\pi}{T} \frac{L}{L_B} \\ I_{p-p} &= 2I_p \sim 1520 A \end{aligned} \quad (7)$$

STRAY FIELD MEASUREMENTS AND SIMULATION

Top-up mode operation of the TPS will face injection transient fields from four-bump kicker and two septum magnets. The kicker magnets excite the stored beam during $\sim 6 \mu\text{sec}$ at the peak of the septa half wave of $\sim 370 \mu\text{sec}$. The betatron motion of the circulating beam

will be excited at the 105th turn along the septum pulse at the rising edge of the kicker magnet pulse, if the leakage field of septums can be neglected. Figure 2(a) illustrates the durations and triggers relationship between the kicker and septum magnets. The black and blue lines show the pulsed signals from kicker and septum magnets, respectively, while Fig. 2(b) shows the layout of the injection section and the eddy current loop in the red frame. Figure 3(a) shows a top-view photo of the TPS injection section, where the right-hand side is the SR and the left-hand side is the transfer line. We utilized mu-metal foils to wrap up the SR beam chamber and minimize the leakage fields to the SR chamber. Figure 3(b) is a photo of eddy current measurements and 3(c) shows the measured eddy currents using two current transformers. We detected a bipolar transmitted current up to 758 amperes by using a current transformer around the vacuum chamber near the upstream septum magnet (SP1) shown as the blue curve in Fig. 3(c). The blue curve shows partial ground currents of 160 A via a short copper cable. Nevertheless, the induction currents are induced by the septum magnet acting like a power source. More parallel current loops could extract larger total currents from the septum magnet power supply. The current loop near the septum magnet is clearly shown on the eddy current measurement.

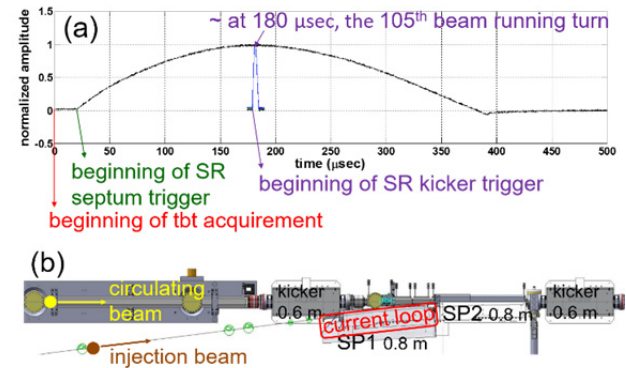


Figure 2: (a) time-relation scheme of septum (black) and kicker magnets (blue), (b) layout of the injection section.

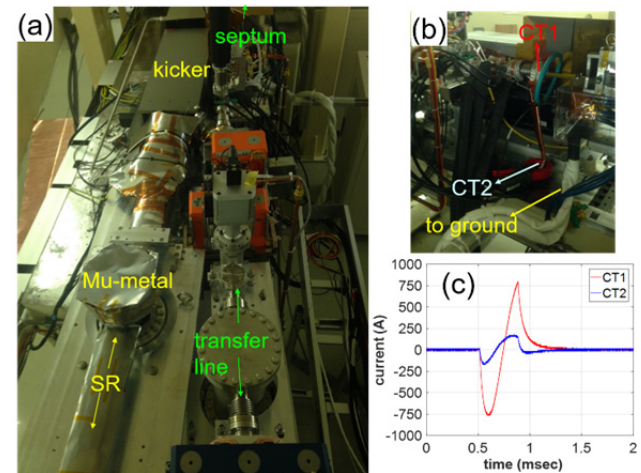


Figure 3: (a), (b) photos of the injection section and (c) eddy current measurements in the real machine.

We mimic the arrangement of a closed circuit using the same septum magnet in the laboratory. A copper wire is connected to the septum and SR vacuum chamber. The pulsed excitation current induces an eddy current on the chamber forming a current loop. The total excited current increases with the numbers of possible current loops due to the lower resistance of parallel resistors. Figure 4 shows that three equal length current loops connected in parallel (blue) increasing the eddy current by 50 % in this experiment.

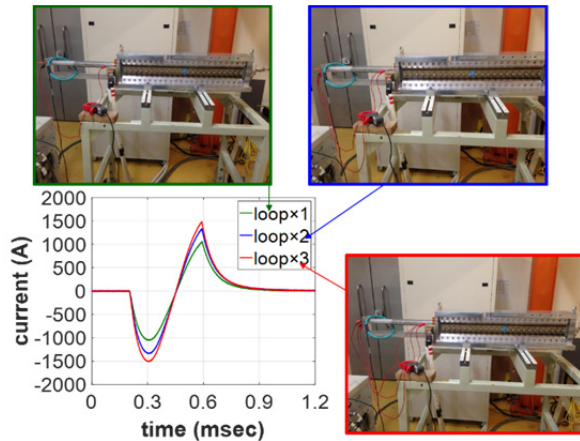


Figure 4: eddy current simulation for different numbers of parallel current loops.

BEAM COD AND FIELD MEASUREMENT AFTER IMPROVEMENT

The circulating beam orbit will be periodically perturbed during top-up injection. Taking turn-by-turn BPM signals is a typical way to further diagnose the betatron motion and stray magnetic fields. We recorded the beam displacements with best matched kickers' fields during the stray field improvement process. In Fig. 5, the measurement employed one of the 172 SR BPMs near the injection section. We recorded the betatron variation before improvement, after mu-metal shielding with cable grounding and current loop isolation. The data were taken during 500 turns within the septum magnet half cycle. During the initial TPS commissioning, there was little shielding outside of the SR vacuum chamber and little grounding to block stray fields causing serious betatron motions as shown in the green line of Fig. 5. We first wrapped mu-metal foils on the SR chamber near the kicker and septum magnets which substantially blocked the leakage field into the SR chamber. The girder is a large mechanical support structure with a low resistivity between beam devices and ground and we therefore use short copper cables to connect the vacuum chambers of the beam transfer line to the girders near the septum magnet. From Eq. (7), we concluded that a long current path in the vacuum chamber should be established to achieve low induced eddy currents, which could be reduced three-fold. Furthermore, we eliminated the possibility of current loops and isolated the current path in the septum chamber. This scheme strongly reduced the eddy current by a factor of 250 in the septum chamber.

The insert in Fig. 5 shows that the eddy current is now less than 3-A in the septum chamber. After improving the stray field, the red line in Fig. 5(b) shows the horizontal and vertical beam displacements to be within peak to peak $\pm 400 \mu\text{m}$ and $\pm 100 \mu\text{m}$, respectively. Comparison of beam orbit perturbations before and after improvements show that the betatron horizontal and vertical displacements decreased by a factor of ten and four, respectively.

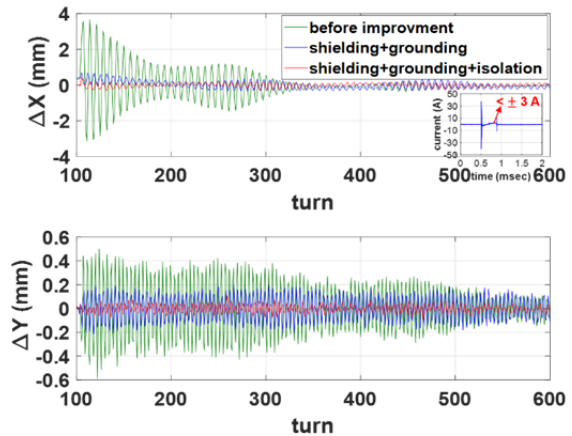


Figure 5: Turn-by-turn BPM data with best matched kicker show betatron oscillations before improvement (green), after mu-metal shielding and grounding with copper cables (blue) and after isolation of current loops (red). The figure insert shows the eddy current after improvements.

CONCLUSION

From a simple model for eddy currents based on Ampere's law, we estimated a 1520 A peak to peak eddy current in the septum chamber. This estimate is approximately equal to the measured eddy current of 1516 A in the real machine.

In order to retain the quality of low photon intensity fluctuations, preserving a good beam orbit stability is necessary. We presented methods to reduce stray fields from septum magnets: by shielding materials surrounding the SR chamber, by adding ground cables from the septum chamber and by breaking multiple current loops, thus improving beam distortion during injection. Preliminary experimental results show an improvement of the beam displacement down to peak to peak $\pm 400 \mu\text{m}$ in the horizontal and peak to peak $\pm 100 \mu\text{m}$ in the vertical plane so far. We will slightly adjust the rotation of the kicker magnets to compensate for vertical betatron displacements. Optimization of kicker-matching and shimming kicker magnets are future plans towards better beam stability during injection.

ACKNOWLEDGMENTS

Authors highly appreciate the technological supports from Instrumentation & Control, Vacuum, Magnet and Precision Mechanical Engineering Groups at NSRRC. We also thank Prof. Humlt Wiedemann to proofread this paper.

REFERENCES

- [1] M. S. Chiu, *et al.*, “The commissioning of phase1 insertion devices in TPS”, in *Proc. IPAC’16*, paper THPMB050.
- [2] Y. Shoji and K. Kumagai, “Stray field of a pulse septum induced by eddy currents”, *IEEE Transactions on Applied Superconductivity*, Vol. 14, Issue: 2, 2004.
- [3] P. Lebasque *et al.*, “Eddy current septum magnets for booster injection and extraction, and storage ring injection at synchrotron SOLEIL”, in *Proc. EPAC06*, paper THPLS101.
- [4] P. Lebasque *et al.*, “Improvement on pulsed magnetic systems at SOLEIL”, in *Proc. EPAC08*, paper WEPC081.
- [5] C. K. Chan *et al.*, “Design and fabrication of the vacuum systems for TPS pulsed septum magnets”, *Nuclear Instruments and Methods in Physics Research A*, 763388–393, 2014.
- [6] D. A. Edwards and M. J. Syphers, *An introduction to the physics of high energy accelerators*, John Wiley & Sons, Inc., pp. 111-113, 1993.